



Novel removal of Anthracene from oil-contaminated water by synthesized modified magnetic nano-particles

A. Torabian*, H. Ahmad-Panahi**, G.R. Nabi-Bidhendi*, N. Mehrdadi

Faculty of the Environment, University of Tehran, 25 Ghods St., Enghelab Ave, Tehran, Iran
Azadeht4@yahoo.com

Department of Chemistry, Islamic Azad University, Central Tehran Branch, Payambar Complex, Shahrak-e Gharb, Tehran, Iran

Panahi20002000@yahoo.com

Faculty of the Environment, University of Tehran, 25 Ghods St., Enghelab Ave, Tehran, Iran

Gnabi@ut.ac.ir

Faculty of the Environment, University of Tehran, 25 Ghods St., Enghelab Ave, Tehran, Iran

nmehrdadi@ut.ac.ir

ABSTRACT

Novel magnetic nanoparticles (MNPs) modified with (3-mercaptopropyl)-trimethoxysilane (MPTMS), grafted with allyl glycidyl ether and coupled with beta naphthol, were prepared for removal of anthracene in aqueous solutions. The grafted MNPs were characterized by transmission electron microscopy (TEM), infrared spectroscopy (FT-IR) and thermogravimetric analysis (TGA). The modified MNPs contributed to enhancement of the adsorption capacity and were prepared by co-precipitation. The modified MNPs were characterized by TEM, FT-IR and TGA and the adsorption and kinetic behavior of anthracene on the modified MNPs was examined. It was shown that the nano-adsorbent optimized adsorption capacity is at pH 7. Three kinetics models: pseudo-first-order, pseudo-second-order, and intraparticle diffusion were used to investigate the adsorption mechanism of the anthracene onto the modified MNPs. The best fit was obtained for the pseudo-second-order model. The synthesized nano adsorbent can be considered as a new method for anthracene adsorption in contaminated water with the benefit of fast removal by applying a magnetic field.

Keywords

Anthracene; Magnetic nanoparticles; Kinetic study; Modification

Council for Innovative Research

Peer Review Research Publishing System

Journal: Journal of Advances in Chemistry

Vol. 10, No. 2

editorjaconline@gmail.com

www.cirjac.com



INTRODUCTION

Anthracene (ANT) is one of a group of chemicals called polycyclic aromatic hydrocarbons (PAHs). PAHs are often found in groups of two or more; they can exist in over 100 different combinations, but the most common are treated as a group of 15. PAHs are found naturally in the environment but can also be man-made. ANT can vary in appearance from a colorless to pale yellow crystal-like solid. ANT, like other PAHs, are created when products like coal, oil, gas, and garbage are burned, but the burning process is not complete. ANT is used to make dyes, plastics, pesticides, smoke screens and scintillation counter crystals. Exposure of the skin to contaminated soil or products like heavy oils, coal tar, roofing tar, or creosote where PAHs have been found can have adverse health effects. Creosote is an oily liquid found in coal tar and is used to preserve wood. Once in the body, ANT can spread and target fat tissues and organs, including the kidneys and liver.

Recent interest in nano-materials comes from their physical and magnetic properties, especially their nano size. Using the magnetic effect of certain types of nano-particles has simplified the process of separating, removing/isolating chosen components from a sample solution. Nano-sized magnetic iron oxide particles have been studied as a new adsorbent with a large surface area and small diffusion resistance [1] for the separation and removal of chemical species such as metals [1-7], dyes [8-10], and gases [1]. Considerable attention has been paid to the combination of organic groups and inorganic magnetic Fe₃O₄ particles at the nano-sized level because of their high specific surface area and the absence of internal diffusion resistance compared to traditional micron-sized supports [11, 12]. It is easy to change the chemical characteristics of the adsorbent surface by chemical modification of the surface. Surface-modified adsorbents can show higher attraction to some substances.

In this study, MNPs were synthesized and grafted with functional monomer and coupled with beta-naphthol. The coupled-grafted MNPs (CGMMNPs) showed a high adsorption capacity for ANT and could be easily separated out from the sample solution using an external magnetic field. This research evaluated the adsorption potential of CGMMNPs for ANT. The kinetic adsorption studies were processed to understand the adsorption mechanism of ANT onto CGMMNPs. Kinetic data was used to calculate the rate at which the object particle was removed from the aqueous solution.

MATERIALS AND METHODS

Materials

1, 4-Dioxane, 2-naphthol, NaCl, C₂H₅OH, CH₃COOH, FeCl₂·4H₂O, FeCl₃·6H₂O, NH₄OH, C₁₄H₁₀, C₁₆H₁₀ were purchased from Merck (Darmstadt, Germany). N, N-Dimethylformamide (DMF), 3-mercaptopropyltrimethoxysilane (MTPMS), allyl glycidyl ether (AGE) and 2, 2-azoisobutyronitrile (AIBN), were purchased from Aldrich (Steinheim, Germany). Anthracene was purchased from Fluka Chemical (Buchs, Switzerland); the molecular structure of ANT is shown in Fig. 1. All the reagents were of analytical grade and used without further purification. The stock solution (2000 mgL⁻¹) of ANT was prepared by dissolving appropriate amounts of ANT in distilled water. For pH adjustment of the solution, 10 ml of 0.1 M acetic acid-acetate buffer (pH 3–6.5) was used wherever required.

Synthesis and surface grafting of magnetite nanoparticles

The MNPs were prepared using chemical co-precipitation by adding ammonia drop-wise to a FeCl₂·4H₂O and FeCl₃·6H₂O solution while injecting nitrogen gas for 30 min. The reaction was carried out at 80°C for 2 h. While the ammonia was added, the color of the solution went from its original brown to dark black, indicating the preparation of MNPs.

The second step was modification of the MNPs. The washed MNPs were dried for 24 h and then silylated using an anhydrous solution of 5% MPTMS in 1, 4-dioxane. The reaction was done in a 1-necked round-bottom flask (equipped with a condenser) at the solution boiling point for approximately 24 h. The modified MNPs (MMNPs) were washed several times with 1, 4-dioxane and dried. The MMNPs and MPTMS were transferred to a degassed graft-polymerization solution containing ethanol as a solvent, AGE, and AIBN as an initiator for 6 h at 70°C. The grafted MMNPs (GMMNPs) were then separated out using a magnetic field, washed, and dried.

The final step was coupling 2-naphthol onto the GMMNPs. This reaction was done by adding the GMMNPs and 2-naphthol dissolved in DMF into a temperature-controlled reactor. The reaction was completed in 8 h at room temperature. The coupled GMMNPs were separated out using a magnetic field, washed, and dried. The aromatic rings of 2-naphthol enabled the adsorption by π-π reactions between benzo(a)pyrene and coupled-grafted-modified MNPs (CGMMNPs). A complete schematic of the synthesis is shown in Fig. 2.

The new CGMMNPs applied as nano-adsorbents were characterized using FT-IR and scanning electron microscopy (TEM).

Adsorption studies

The adsorption of ANT by the CGMMNPs (as a magnetic nano-adsorbent) was studied by batch equilibrium in an aqueous solution. For the adsorption experiments, stock aqueous solutions of ANT were prepared by dissolving the proper amount of ANT in twice-distilled water. The initial stock solution was 2000 mgL⁻¹, and the secondary stock solution was 0.8 mgL⁻¹. The effect of pH was studied for a range of 4 to 8. For each experiment, 0.02 g of adsorbent was poured into a beaker and mixed with 10 ml of secondary solution. The pH values were adjusted to the desired value in range of the buffer solutions (0.01 M acetate and/or 0.01 M phosphate). The final solution was shaken for 10 min at room temperature. Afterward, the magnetic nano-adsorbents were removed using a magnetic field and the remaining supernatant ANT concentration was



measured using HPLC (Agilent 1100 series). The amount of ANT at equilibrium q_e (mg g⁻¹) on the CGMMNPs was calculated as:

$$(1) q_e = (C_0 - C_e) V/W$$

Where C_0 and C_e (mg/l) are the initial and equilibrium ANT concentrations, respectively, V is the volume of the ANT solution, and W (g) is the mass of the adsorbent.

The kinetic study of ANT adsorption onto CGMMNPs was done by applying the same experimental procedure described above. Different beakers containing ANT solution and 0.02 of nano-adsorbent were shaken for different time intervals; as in previous experiments, the optimum pH was 7. Adsorption was determined by:

$$(2) qt = (C_0 - C_t) V/W$$

Where C_0 and C_t (mg/l) are the ANT concentrations initially and at each time interval, respectively, V is the volume of the ANT solution, and W (g) is the mass of the nano-adsorbent.

RESULTS AND DISCUSSION

The characterization of copolymer-grafted magnetic nanoparticles

The CGMMNPs were characterized by transmission electron microscopy (TEM), infrared spectroscopy (FT-IR) and thermogravimetric analysis (TGA). The FT-IR spectrum for the CGMMNPs was compared with the raw MNPs as well as FT-IR: (NaCl, cm⁻¹) 3779.8 (OH), 1627 (C=O), 1450 (aromatic cycle), 3051.53 (aromatic C-H) and 1000 (C-O). The presence of an aromatic group in the FT-IR spectrum of the CGMMNPs indicates that coupling of the 2-naphthol was performed successfully. The TGA of the unmodified MNPs indicated that weight loss up to 120°C was caused by water molecule desorption from the surface; after 200°C, the weight remained constant.

GMNPs, however, showed completely different thermal behavior. Weight loss up to 200°C was caused by the water molecules in the grafted MNPs and the weight loss at 220 to 500 °C, was because of the decomposition and desorption of the polymeric matrix Fig. 3. These results demonstrate the formation of CGMMNPs. The FT-IR spectrum and TGA confirmed the structure of the grafted polymer. TEM was used to examine the external surface of the CGMMNPs. As shown in Fig. 4, the particles were spherical with a rough surface and the particle size was 15-40 nm.

Effect of pH on ANT adsorption

The effect of pH was studied for a range of 4-8 Fig. 5. The studies showed that pH played a critical role in the adsorption process. An appropriate pH value increased the adsorption effectiveness and decreased interference with the matrix. The adsorption of ANT in solution decreased as the pH of the aqueous solution increased from 4 to 5. At pH =7, optimum adsorption was achieved, suggesting a neutral pH for adsorption. At this pH, no precipitation occurred; pH values above 8 were not considered because of their effect on CGMMNP structure.

Adsorption kinetics

Fig. 6 shows the adsorption kinetics of ANT onto CGMMNPs. The kinetic study indicated that 10 min was sufficient for complete adsorption. The profile of ANT uptake by the CGMMNPs showed good accessibility of the active sites on the nano-adsorbent surface. The adsorption kinetics of ANT onto the CGMMNPs was done using pseudo-first-order and pseudo-second-order kinetic equations. The pseudo-first-order equation is:

$$(3) \log (q_e - q_t) = \log q_e - k_1 t/2.303$$

Where q_e and q_t (mg/g) are the amount of adsorbed ANT at equilibrium and at time t , respectively, and k_1 is the rate constant of the pseudo-first-order (1/min). As shown in Fig. 7, a straight line resulted from the plot of $\log (q_e - q_t)$ versus t where k_1 is the line slope. Table 1 shows the calculated and experimental q_e and R^2 correlations.

The pseudo-second-order equation is:

$$(4) t/q_t = 1/k_2 q_e^2 + t/q_e$$

In this equation, q_e and q_t (mg/g) are the amount of ANT adsorbed onto the CGMMNPs at equilibrium and at time t , respectively, and k_2 is the rate constant of the pseudo-second-order (g/mg min). By plotting t/q_t versus t , a straight line results (Fig. 8) where q_e and k_2 are the slope and intercept of this line, respectively. The values of k_2 , the calculated and experimental q_e , and the correlation coefficients (R^2) are shown in Table 1.

Because of the probability of intra-particle diffusion, the intra-particle diffusion model was used to evaluate the diffusion mechanism of adsorption. The model is represented as:

$$(5) qt = k_p t^{0.5} + C$$

In this equation, C is the intercept and k_p is the slope of intra-particle diffusion (mg/g min^{0.5}). From the plot of qt versus t , a straight line results (Fig. 9). The values of k_p , C , and R^2 are shown in Table 1. If the line does not pass through the origin, it means that intra-particle diffusion is not the only rate-limiting process, and the relationship between qt and $t^{0.5}$ is not linear. Other rate-controlling steps can be explained by the boundary layer effect. As seen in Table 1 the calculated q_e value for the pseudo-second-order kinetics agrees with the experimental q_e value and its correlation coefficient was greater than 0.99 This shows that the pseudo-second-order kinetics model well described the adsorption kinetics. It can be



concluded that this kind of grafted magnetic adsorbent in low amounts shows selectivity for the ANT. Compared with the conventional adsorption process, the magnetic separation method has advantages such as ease of operation, cost effectiveness, high selectivity, and rapid separation.

CONCLUSION

A method is introduced in this study for graft polymerization of MNPs and coupling it with an aromatic compound as a novel adsorbent. The nano-adsorbent showed good potential for fast removal of PAHs from large sample volumes and possessed advantages such as of high adsorption capacity and high chemical stability. The optimized capacity was achieved at pH 7 and the equilibrium time was 10 min.

On the basis of Langmuir isotherm analysis, the monolayer adsorption capacity was determined to be $4.17 \text{ (mg g}^{-1}\text{)}$ at 20°C . Pseudo-first-order, pseudo-second-order, and intra-particle diffusion were kinetic models used to determine the adsorption mechanism of ANT onto CGMMNPs. The best fit was achieved by the pseudo-second-order model; therefore, this type of modified nanoparticle can be introduced as a low-cost and effective adsorbent for ENR adsorption from aqueous solutions.

ACKNOWLEDGMENTS

The authors appreciate the support provided University of Tehran,

REFERENCES

- [1] Liao MH, Chen D. Fast and efficient adsorption/desorption of protein by a novel magnetic nano-adsorbent *Biotechnology Letters* 2002;24:1913-7.
- [2] Faraji M, Yamini Y, Rezaee M. Extraction of trace amounts of mercury with sodium dodecyl sulphate-coated magnetite nanoparticles and its determination by flow injection inductively coupled plasma-optical emission spectrometry. *Talanta* 2010;81:831-6.
- [3] Huang C, Hu B. Silica-coated magnetic nanoparticles modified with γ -mercaptopropyltrimethoxysilane for fast and selective solid phase extraction of trace amounts of Cd, Cu, Hg, and Pb in environmental and biological samples prior to their determination by inductively coupled plasma mass spectrometry. *Spectrochimica Acta Part B: Atomic Spectroscopy* 2008;63:437-44.
- [4] Macdonald J, Kelly J, Veinot J. Iron/Iron Oxide Nanoparticle Sequestration of Catalytic Metal Impurities from Aqueous Media and Organic Reaction Products. *Langmuir* 2007;23:9543-5.
- [5] Mayoa JT, Yavuz C, Yeanb S, Congb L, Shipleyb H, Yua W, et al. The effect of nanocrystalline magnetite size on arsenic removal. *Science and Technology of Advanced Materials* 2007;8:71-5
- [6] Uheida A, Alvarez G, Björkman E, Yu Z, Muhammed M. Fe_3O_4 and $\gamma\text{-Fe}_2\text{O}_3$ nanoparticles for the adsorption of Co^{2+} from aqueous solution. *Journal of Colloid and Interface Science* 2005;298:501-7.
- [7] Wang L, Yang Z, Gao J, Xu K, Gu H, Zhang B, et al. A Biocompatible Method of Decorporation: Bisphosphonate-Modified Magnetite Nanoparticles to Remove Uranyl Ions from Blood. *Journal of the American Chemical Society* 2006;128:13358-9.
- [8] Chang Y, Chen D. Adsorption Kinetics and Thermodynamics of Acid Dyes on a Carboxymethylated Chitosan-Conjugated Magnetic Nano-Adsorbent. *Macromolecular Bioscience* 2005;5:254-61.
- [9] Faraji M, Yamini Y, Saleh A, Rezaee M, Ghambarian M, Hassani R. A nanoparticle-based solid-phase extraction procedure followed by flow injection inductively coupled plasma-optical emission spectrometry to determine some heavy metal ions in water samples. *Analytica Chimica Acta* 2010;659:172-7.
- [10] Yang N, Zhu S, Zhang D, Xu S. Synthesis and properties of magnetic Fe_3O_4 -activated carbon nanocomposite particles for dye removal. *Materials Letters* 2008;62:645-7.
- [11] Goswamia R, Debb P, Thakurc R, Sarmaa KP, Basumallickd A. Removal of As(III) from aqueous solution using functionalized ultrafine iron oxide nanoparticles, . *Separation Science and Technology* 2011;46:1017-22.
- [12] Li Z, Sun Q, Gao M. Preparation of Water-Soluble Magnetite Nanocrystals from Hydrated Ferric Salts in 2-Pyrrolidone: Mechanism Leading to Fe_3O_4 . *Angewandte Chemie International Edition* 2004;44.

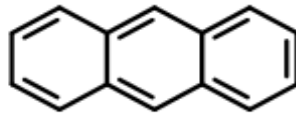


Fig 1:Anthracene molecule structure

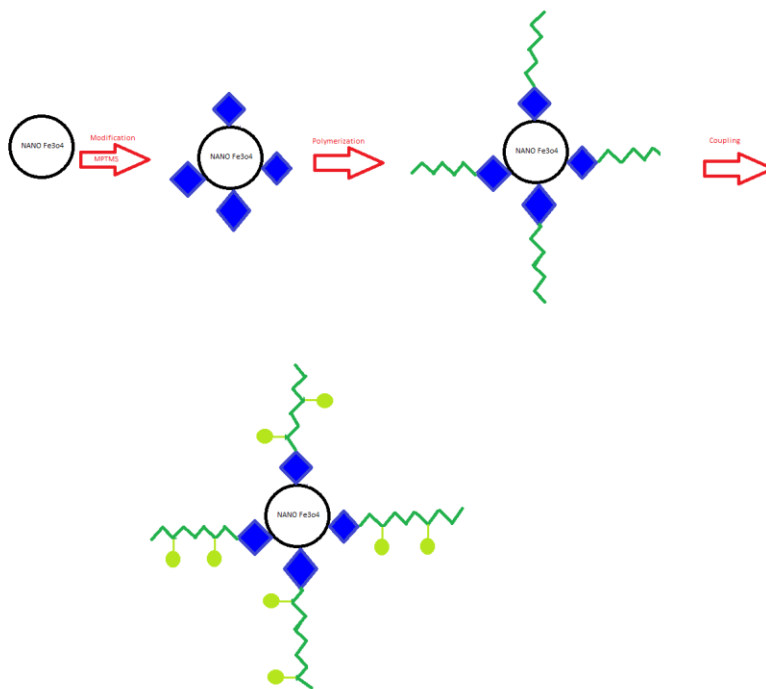
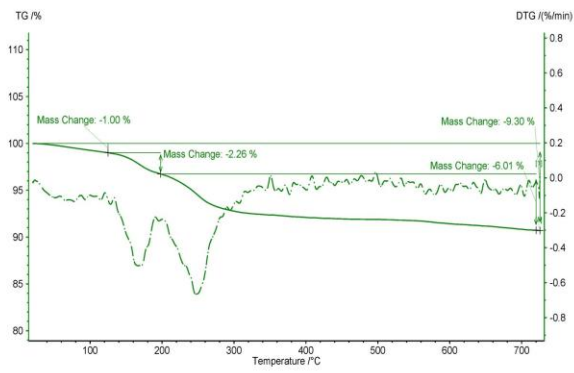
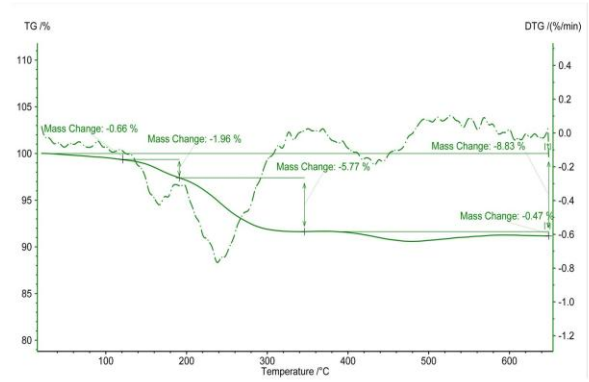


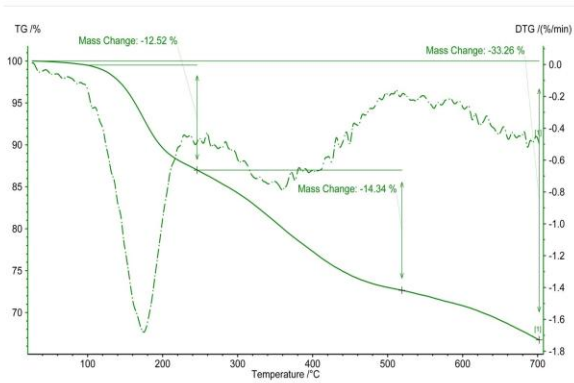
Fig 2: Schematic presentation of silylation, graft polymerization and coupling of grafted magnetic nano particles



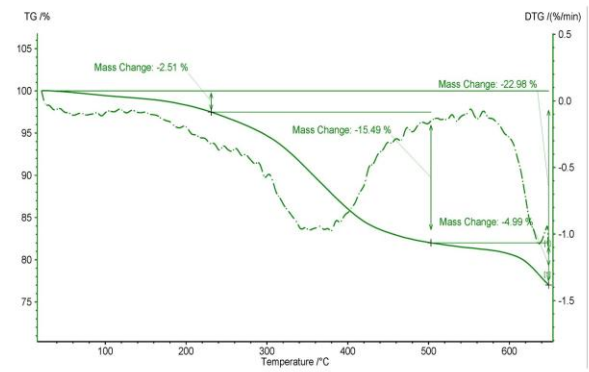
a



b



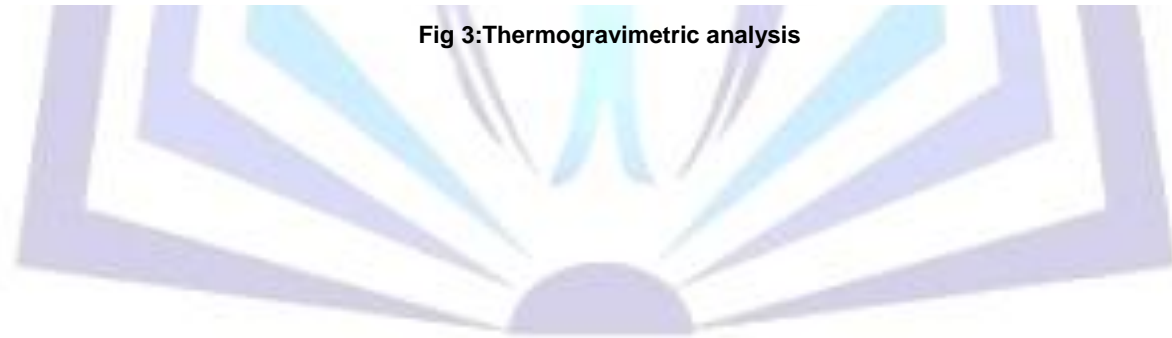
c



d

Fig. 3. Thermogravimetric analysis of MNPs (a), modified MNPs (b), grafted MNPs (c) CGMMNPs (d)

Fig 3:Thermogravimetric analysis



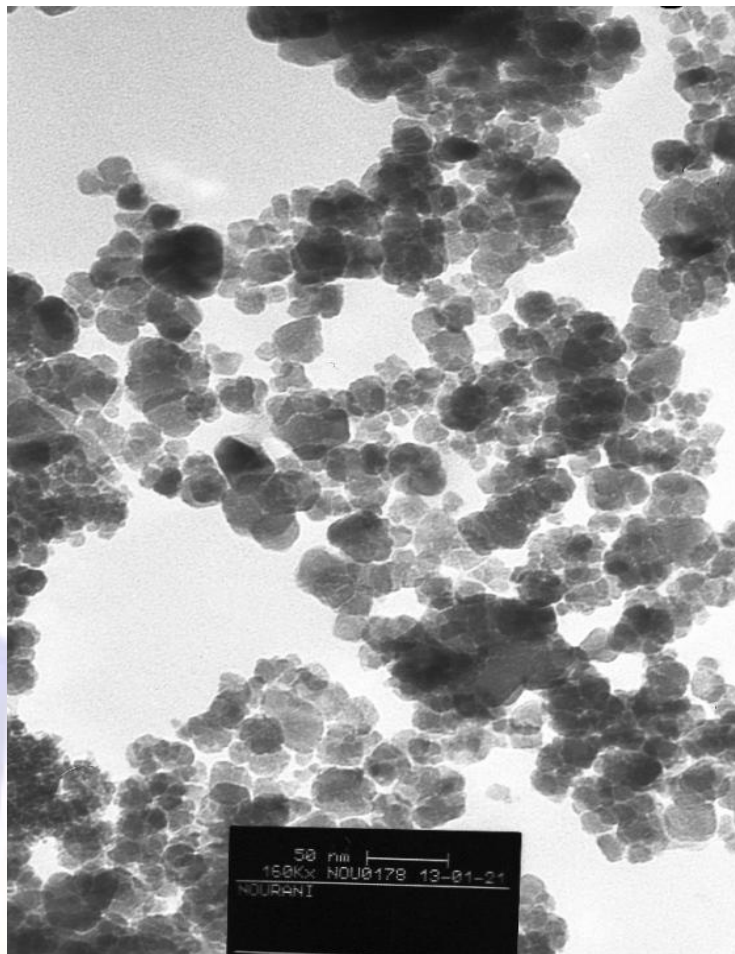


Fig 4:TEM image

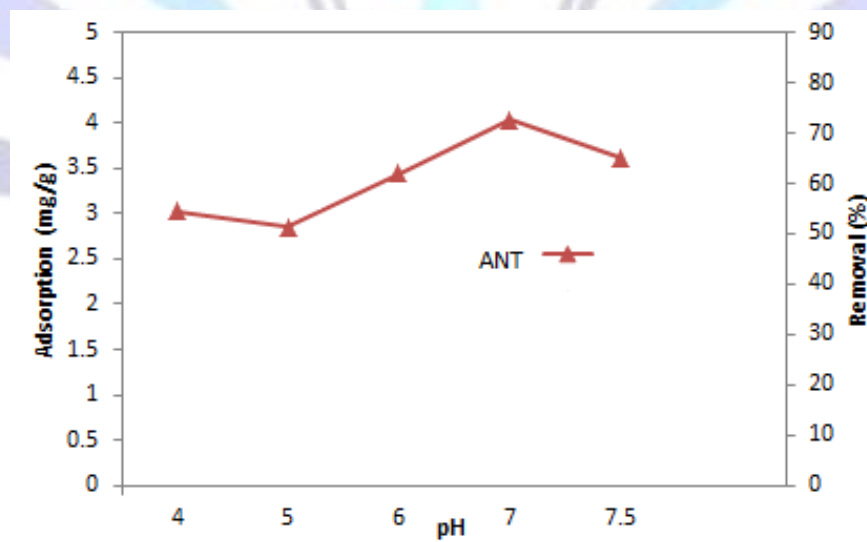


Fig 5:Effect of pH on adsorption of ANT on CGMMNPs

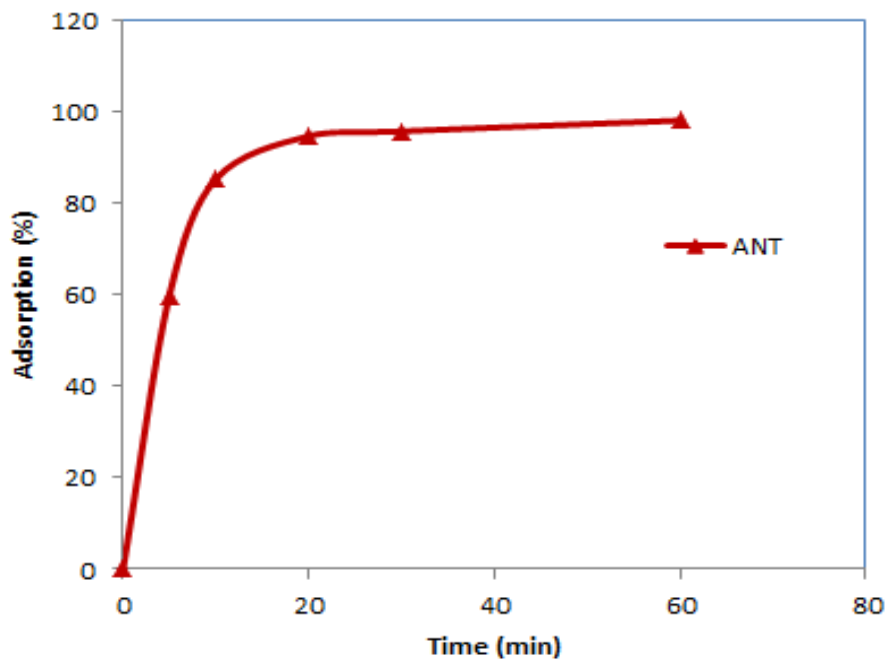


Fig 6: The kinetic study of ANT removal

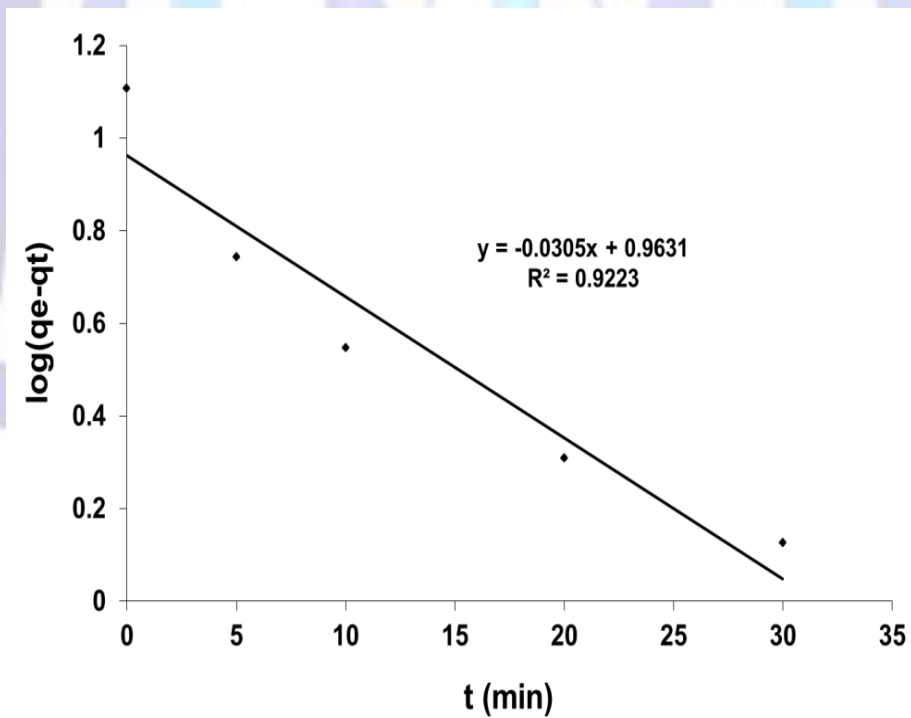


Fig 7: The pseudo - first -order kinetics for ANT adsorption by CGMMNPs

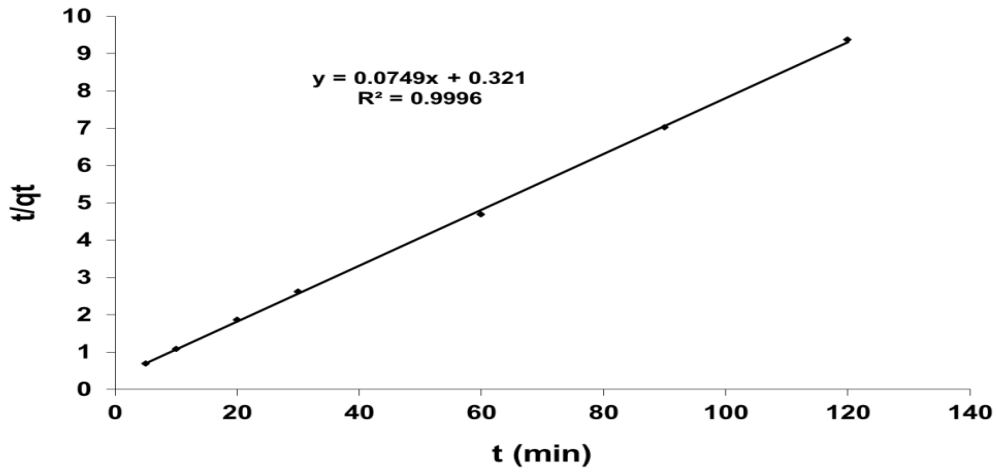


Fig 8: The pseudo-second-order kinetics for ANT adsorption by CGMMNPs

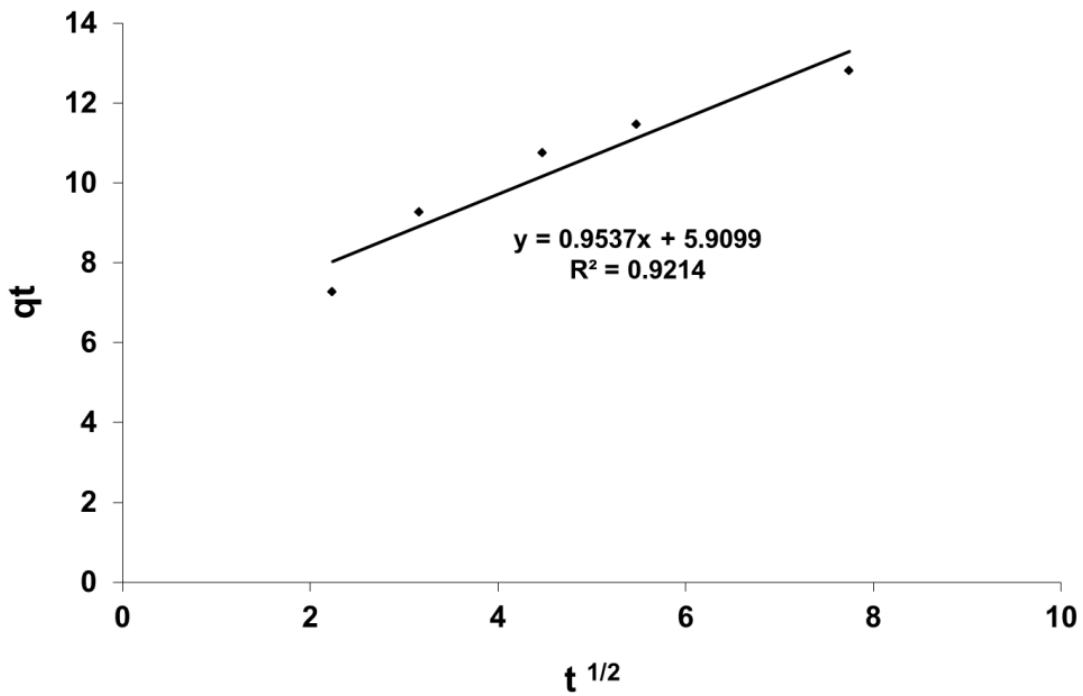


Fig 9: Intraparticle diffusion kinetics for ANT adsorption by CGMMNPs



Kinetic Models	
pseudo-first-order	
<i>q_e</i> (mg/g)	9.183
<i>k</i> ₁	0.070
R ²	0.922
pseudo-second-order	
<i>q_e</i> (mg/g)	13.35
<i>K</i> ₂	0.017
R ²	0.921
Intraparticle diffusion	
<i>k_p</i> (mg/g min ^{0.5})	0.953
<i>C</i>	5.909
R ²	0.921

Table 1: Comparison of the pseudo-first-order, pseudo-second-order and intraparticle diffusion models calculated equilibrium, rate constants and correlation coefficients

